RhoH is critical for cell-microenvironment interactions in chronic lymphocytic leukemia in mice and humans

Anja Troeger,[1,2] Amy J. Johnson,[3,4] Jenna Wood,[1] William G. Blum,[3] Leslie A. Andritsos,[3] John C. Byrd,[3,4] and David A. Williams[1]

[1]Division of Hematology/Oncology, Children's Hospital Boston, Boston, MA; [2]Clinic for Pediatric Oncology, Hematology, and Clinical Immunology, Heinrich Heine University Duesseldorf, Duesseldorf, Germany; and [3]Division of Hematology, Department of Medicine, and [4]Division of Medicinal Chemistry, College of Pharmacy, Ohio State University, Columbus, OH

Trafficking of B-cell chronic lymphocytic leukemia (CLL) cells to the bone marrow and interaction with supporting stromal cells mediates important survival and proliferation signals. Previous studies have demonstrated that deletion of *Rhoh* led to a delayed disease onset in a murine model of CLL. Here we assessed the impact of RhoH on homing, migration, and cell-contact dependent interactions of CLL cells. *Rhoh*$^{-/-}$ CLL cells exhibited reduced marrow homing and subsequent engraftment. In vitro migration toward the chemokines CXCL12 and CXCL13 and cell-cell interactions between *Rhoh*$^{-/-}$ CLL cells and the supporting microenvironment was reduced. In the absence of RhoH the distribution of phosphorylated focal adhesion kinase, a protein known to coordinate activation of the Rho GTPases RhoA and Rac, appeared less polarized in chemokine-stimulated *Rhoh*$^{-/-}$ CLL cells, and activation and localization of RhoA and Rac was dysregulated leading to defective integrin function. These findings in the *Rhoh*$^{-/-}$ CLL cells were subsequently demonstrated to closely resemble changes in GTPase activation observed in human CLL samples after in vitro and in vivo treatment with lenalidomide, an agent with known influence on microenvironment protection, and suggest that RhoH plays a critical role in prosurvival CLL cell-cell and cell-microenvironment interactions with this agent. (*Blood*. 2012; 119(20):4708-4718)

Introduction

In patients with chronic lymphocytic leukemia (CLL) the characteristic accumulation of monoclonal mature B lymphocytes in the peripheral blood (PB), bone marrow (BM), and secondary lymphoid tissues (SLTs) is mostly attributed to defective in vivo apoptosis, whereas these cells undergo rapid cell death in vitro.[1,2] It has been demonstrated that ex vivo coculture of CLL cells with stromal cells enhances their survival, and a fraction of CLL cells proliferate in close contact with T lymphocytes and stromal cells within pseudofollicles.[3] Therefore, close contact to accessory cells in the BM and SLTs may contribute to their sustained in vivo survival.[2] This is further supported by the observation that CD38 expression associated with adverse outcome in CLL is up-regulated in response to activated T cells, and thus increased in tissues containing pseudofollicles.[4] In long-term in vitro cultures of PB mononuclear cells (PBMNCs) from CLL patients, an adherent cell population, called "nurse-like" cells (NLCs) can be obtained.[5] These NLCs express and produce chemokines, such as CXCL12 and CXCL13, which regulate trafficking of human CLL cells between PB, lymphoid organs, and BM, and thus promote interaction with the microenvironment necessary for their survival and proliferation.[6,7] Furthermore, matrix metalloproteinase-9 is up-regulated in response to integrin, CXCL12, and CCR7 signaling via Erk activation in CLL cells and regulates migration and lymph node infiltration thereby contributing to disease progression.[8]

Trafficking, directed migration and homing are complex processes that involve the coordinate activation of Rho GTPases, such as Rac and RhoA downstream of integrins, and chemokine receptors in lymphocytes.[9] Their activity varies in a cell and agonist-specific fashion and is dependent in part on their intracellular localization.[10] In this regard, the Src nonreceptor tyrosine kinase and its target focal adhesion kinase (FAK) are critical regulators of both RhoA and Rac.[11]

RhoH, a hematopoietic-specific member of the RhoE/Rnd3 subfamily of GTPases was initially identified as hypermutable gene and translocation partner in human B-cell lymphomas suggesting its involvement in the pathogenesis of B-cell malignancies.[12-15] *Rhoh*$^{-/-}$ mice exhibit a profound T-cell defect because of impaired T-cell receptor (TCR)–mediated selection and maturation of thymocytes as RhoH is required for CD3ζ phosphorylation and recruitment of the protein tyrosine kinases Zap70 and Lck to the cellular membrane and immunologic synapse.[16-19]

Although the functional importance of RhoH has been well defined in T cells, its role in B-cell development appears less clear. However, in human CLL samples RhoH expression correlates with expression of the unfavorable prognostic marker Zap70. We previously reported an attenuated disease onset in the absence of RhoH in an *Eμ-TCL1*^{Tg} mouse model of CLL,[20] which seemed paradoxical given the lack of RhoH involvement in normal B-cell development and the severe T-cell immune deficiency exhibited in *Rhoh*$^{-/-}$ mice.[16] *Eμ-TCL1*^{Tg}*;Rhoh*$^{-/-}$ mice were characterized by a significantly reduced number of CLL cells in the BM, but the cell autonomous basis of RhoH effects in this disease model were not clearly delineated. Whereas reduced numbers of CLL cells in *Eμ-TCL1*^{Tg}*;Rhoh*$^{-/-}$ mice may represent cell-autonomous

Submitted November 30, 2011; accepted March 18, 2012. Prepublished online as *Blood* First Edition paper, April 3, 2012; DOI 10.1182/blood-2011-12-395939.

The online version of this article contains a data supplement.

The publication costs of this article were defrayed in part by page charge payment. Therefore, and solely to indicate this fact, this article is hereby marked "advertisement" in accordance with 18 USC section 1734.

alterations in survival or proliferation, the unequal distribution of CLL cells within the different compartments in the absence of RhoH suggests that RhoH may be involved in chemokine-mediated CLL trafficking processes.

Here we investigated the impact of RhoH deletion on CLL cell homing and migration, NLC-interaction and downstream biochemical events after chemokine stimulation in the *Eμ-TCL1*^{Tg};*Rhoh*$^{-/-}$ mouse model. *Rhoh*$^{-/-}$ CLL cells were characterized by reduced in vitro chemotaxis, which correlated with a decreased in vivo homing of CLL cells to the BM. In addition, cell-cell interaction of CLL cells with NLC was reduced in the absence of RhoH. RhoH deficiency also resulted in an altered pattern of RhoA and Rac activation that was strikingly similar to changes observed after treatment of primary human CLL cells with lenalidomide providing a potential mechanism for this agent's ability to influence CLL cell survival. Taken together, these observations suggest that RhoH plays a critical role in CLL progression at least in part via regulation of cell-cell interactions and resulting failure of the microenvironment in *Rhoh*$^{-/-}$ mice or in lenalidomide treated humans to support survival of CLL cells in vivo.

Methods and Materials

Mice

The generation of a murine model that closely resembles human CLL has been previously described. To study the role of RhoH in leukemogenesis, *Eμ-TCL1*^{Tg}*;Rhoh*$^{+/+}$*(Eμ-TCL1*^{Tg};*WT*) and *Eμ-TCL1*^{Tg};*Rhoh*$^{-/-}$ mice were backcrossed to a C57BL/6J background.[20,21] *Rag2*$^{-/-}$ *IL2γ*$^{-/-}$ recipient mice used in transplantation experiments were obtained from Taconic. All animal procedures and experiments were approved by the Institutional Animal Care and Use Committee of Children's Hospital Boston.

Histology preparations

Hematoxylin and eosin (H&E) staining and immunohistochemistry staining for Mac-2 expression was performed on spleens from diseased *Eμ-TCL1*^{Tg}*;WT* and *Eμ-TCL1*^{Tg};*Rhoh*$^{-/-}$ mice applying standard protocols. Slides were evaluated by photomicroscopy at 200× magnification and the percentage of Mac-2^{+} cells in 2 scanned spleen sections per animal determined using ImageScope Version 7.01 software from Aperio Technologies. Spleens from 3 animals/genotype were randomly reviewed.

Isolation of murine CLL cells

Single cell fractions from PB and spleens were obtained according to standard protocols. CLL content of all samples used for outlined functional experiments was verified by flow cytometry to be $>$ 60%-90%. Samples with less than 60% CLL cells were enriched by T-cell depletion using mouse CD90.2 Microbeads and LD columns (Miltenyi Biotec), following the manufacturer's recommendations.

Flow cytometry analysis

After red cell lysis with PharmLyse (BD Bioscience) buffer for 10 minutes, the cell suspensions were incubated for 20 minutes in the dark at 4°C with a 1:100 dilution of the appropriate antibody conjugates in PBS supplemented with 2% FCS for staining. CLL cells were identified as CD3^{-}/CD5^{+}/IgM^{+} cell fraction using CD3ε-FITC (145-2C11), IgM-APC (II/41), and CD5-PE or PE-Cy7 (53-7.3). Normal B cells were defined by positive surface staining for B220-APC-Cy7 (RA3-6B2; BD Bioscience and eBioscience). After a washing step with PBS pellets were resuspended in 200-300 uL PBS/2% FCS for analysis. To identify and exclude dead cells either 7AAD (Invitrogen) or 4′,6-diamidino-2-phenylindole (DAPI; Sigma-Aldrich) was added to the staining solution. Cells were analyzed on a LSRII flow cytometer (BD Bioscience) using BD FACSDiva Version 6.1.1. software (BD Bioscience).

In vivo homing and transplantation assays

Twenty to 25×10^6 CLL cells obtained from the spleens of diseased *Eμ-TCL1*^{Tg}*;WT* and *Eμ-TCL1*^{Tg};*Rhoh*$^{-/-}$ mice were injected into the tail veins of nonirradiated *Rag2*$^{-/-}$*IL2γ*$^{-/-}$ recipient mice. After 16 hours the animals were killed and cell counts obtained from the BM and PB. Both the cellular input as well as cells homing to the BM and remaining in the PB were analyzed by flow cytometry to assess the fraction and total number of CLL cells. The percentage of CD3^{-}/CD5^{+}/IgM^{+}CLL cells homing to the BM or circulating in the blood relative to the total number of input CLL cells were used to describe their homing capacity. For transplantation assays, 2×10^7 CLL cells, again obtained from spleens of diseased *Eμ-TCL1*^{Tg}*;WT* and *Eμ-TCL1*^{Tg};*Rhoh*$^{-/-}$ mice, were injected intraperitoneally into nonirradiated *Rag2*$^{-/-}$*IL2γ*$^{-/-}$ recipient mice and disease progression followed by flow cytometry in the PB. In addition, BM infiltration and spleen weight was assessed in a separate group of animals 3 weeks after transplantation.

In vitro culture of NLCs

MNCs were isolated by density-gradient centrifugation over Ficoll (Histopaque-1083, Sigma-Aldrich) from PB or spleens of diseased *Eμ-TCL1*^{Tg}*;WT* and *Eμ-TCL1*^{Tg};*Rhoh*$^{-/-}$ mice and cultured in RPMI1640 medium supplemented with 10%FCS and 1% penicillin/streptomycin. Equal final concentrations of 5×10^5 to 1×10^7 cells/mL were incubated for 14 and 4 days at 37C and 5% CO_2 in tissue treated plates. Cultures were analyzed by phase-contrast microscopy for the outgrowth of adherent NLCs and colocalizing CLL cells were counted in 2 visual fields at 200× magnification. After 2 weeks the adherent cell fraction was transferred to poly-L-lysine coated slides and stained for expression of anti-CD68 (H-255; Santa Cruz Biotechnology) using anti–rabbit Alexa 488 secondary antibody (Invitrogen) and F-actin with rhodamine (TRITC)–labeled phalloidin (Molecular Probes). Slides were covered with DAPI-containing mounting medium (Vector Laboratories).

Immunofluorescence staining

For immunofluorescence staining, CLL cells were layered onto poly-L-lysine or fibronectin-coated cover slides and in part of the experiments stimulated with 100 ng/mL CXCL12 or 800 ng/mL CXCL13 for 2 minutes at 37°C. Cells were subsequently fixed using BD Cytofix/Cytoperm (BD Bioscience) solution and stained with Rhodamine (TRITC)–labeled phalloidin, anti-Rac1 (BD Bioscience, Transduction Laboratories), anti-RhoA (Santa Cruz Biotechnology) or anti–phospho-FAK (pFAK-Tyr925 or pFAK-Tyr397) antibody (Cell Signaling Technology) followed by anti–mouse Alexa 488 secondary antibody (Invitrogen). XYZ series fluorescence images were captured with a PerkinElmer UltraView Vox Spinning Disc confocal microscope (Nikon) equipped with a 60× objective lens and ultra view molecular laser, connected to a Hamamatsu C9100-50 camera driven by Velocity software (Perkin Elmer). Images were analyzed for colocalization and protein quantification using Velocity Version 5.3.2 (Perkin Elmer) and Image J Version 1.42q software.

Chemotaxis assays

Splenocytes from disease-stage matched animals were isolated and 500 000 cells/well seeded in the upper chamber of 24-well, 5-μm transwell plates (Corning) in triplicate. To assess the influence of ICAM-1 activation on migration, in some assays the filter of the upper chamber was coated with 40 ug/mL recombinant ICAM-1. The lower chamber contained 600 μL of complete medium supplemented with either 100 ng/mL CXCL12 (PeproTech) or 800 ng/mL CXCL13 (R&D Systems). After 4 hours incubation, cells that migrated to the lower chamber were collected and counted using a hemocytometer or Hemovet counter. To assess the number of migrated leukemic cells, flow analysis of both the input as well as the migrated cell fraction was performed. The results were expressed as the percentage of

migrated $CD3^-/CD5^+/IgM^+$CLL cells, relative to the total number of input $CD3^-/CD5^+/IgM^+$CLL cells.

Immunoblotting

For immunoblotting and GTPase activity assays, cells were lysed on ice in Mg^{2+} lysis/wash buffer (Upstate Biotechnology) containing 8% glycerol as well as complete protease inhibitor cocktail (Roche Applied Science) and phosphatase inhibitors (10mM sodium fluoride, 1mM sodium orthovanadate). In part of the experiments CLL cells were stimulated for the indicated time points with 100 ng/mL CXCL12 or 800 ng/mL CXCL13 before cell lysis. To assess Rac and RhoA activity, cellular extracts were incubated with GST-p21–activated kinase (PAK1) or Rhotekin RBD agarose beads (Millipore) as previously described. Activated, GTP-bound Rac and RhoA levels as well as total protein were assessed after separation on 12% sodium dodecyl sulfate (SDS) polyacrylamide gels and transfer to polyvinylidene difluoride membrane (PVDF; BioRad) using anti-Rac1 antibody and anti-RhoA antibody in a 1:1000 dilution. β-actin (AC-15; Sigma-Aldrich) was used as a loading control for total protein levels in a 1:10 000 dilution. The RhoH antibody was previously described,[22] anti–pFAK-Tyr925, anti-pFAK-Tyr397, and anti-FAK were obtained from Cell Signaling Technology. HRP-coupled anti–mouse or anti–rabbit antibodies at a dilution of 1:2000 and LumiGlo chemiluminescent substrate (Cell Signaling Technology) were used for detection.

Human CLL samples

After signed informed consent and approval by the Institutional Review Board of the Ohio State University, human PB samples were collected from CLL patients. PBMNCs were obtained by density-gradient centrifugation over Histopaque (GE Healthcare) and CLL cells further purified before in vitro treatment by Rosette-Sep technique (StemCell Technologies). After a purity of $> 90\%$ for $CD19^+CD5^+$ cells was confirmed by flow cytometry using anti–human CD19-APC (BD Bioscience), aliquots a 1×10^7 of freshly isolated CLL cells were treated with either vehicle or 0.5uM of lenalidomide for the indicated time points. This concentration is attainable with doses ranging from 2.5 to 10 mg daily, although there is variation in pharmacology among patients with this agent. Subsequently cell pellets were frozen and GTPase expression and activity determined by pull down and Western blot analysis after cell lysis as stated above. For examination of the effects of lenalidomide in vivo, samples were obtained from relapsed patients before (pre) and after 8 days (d8) of in vivo treatment with lenalidomide within a phase 1 clinical trial at OSU (NCT00466895). All patients on this trial were at least 4 weeks from receiving their last chemotherapy when lenalidomide treatment was initiated. For analysis, patients were chosen randomly after determining the availability of circulating tumor cells. As severe side effects and tumor flare reactions were observed after high dose treatment (25 mg), patients in this study were started on a lower dose of 2.5 mg lenalidomide. The patients studied received lenalidomide at 2.5 to 5 mg per day for 8 days. Blood samples were collected before therapy and on day 8 (after therapy). PBMNCs at these time points were obtained by density-gradient centrifugation and cryopreserved in dimethylsulfoxide (DMSO) for subsequent analysis. Isolated PBMNCs contained $> 87\%$ $CD19^+$ cells and were not further purified.

Image acquisition

Fluorescence images both in main text and supplemental Figures (see Figures 4A-B, 5C, and supplemental Figures 3 and 8) were taken with a PerkinElmer UltraView Vox Spinning Disc confocal microscope (Nikon Inc) using a 60× objective lens and ultra view molecular laser at room temperature, with oil imaging medium; TRICT, Alexa488, DAPI, EGFP, Alexa594 fluorochromes were used as indicated and acquired with a C9100-50 electron multiplier CCD camera (Hamamatsu Photonics); Velocity software (Perkin Elmer) and Image J software (NIH) were used as acquisition and image processing software.

Tissue culture images (see Figure 2) were taken with a Nikon Eclipse TS100 microscope (Nikon Inc), with a 20× objective lens at room temperature. The camera used was a Nikon Digital Sight (Nikon Inc).

Statistical analysis

To determine differences between BM homing, percentage of Mac-2^+ cells in the spleen sections, as well as for comparison of surface marker MFI values of wild-type (*WT*) and *Rhoh*$^{-/-}$ CLL cells student *t* test and Mann-Whitney *U* (MWU) test was applied. CXCL12 and CXCL13 serum levels were compared in *WT*, *Rhoh*$^{-/-}$, *Eμ-TCL1*^{Tg};*WT*, and *Eμ-TCL1*^{Tg};*Rhoh*$^{-/-}$ mice by Kruskal-Wallis test. For comparison of GTPase expression and activation levels as well as migration before and after in vivo treatment with lenalidomide a paired Student *t* test was used. Survival in transplanted animals was compared by χ^2 test and Kaplan-Meier analysis. Statistical analysis was performed using the PASW statistics 18 program. Two-sided *P* values $\leq .05$ were considered significant.

Results

Significantly reduced BM homing efficiency of *Rhoh*$^{-/-}$ CLL cells in vivo

Genetic knockout of *Rhoh* in the *Eμ-TCL1*^{Tg} mouse model of CLL leads to reduced numbers of CLL cells in the BM and significantly delays disease onset.[20] To determine whether this was because of reduced trafficking and homing of *Rhoh*$^{-/-}$ CLL cells an in vivo homing assay of $CD3^-/CD5^+/IgM^+$ cells generated in *WT* versus *Rhoh*$^{-/-}$*;Eμ-TCL1*^{Tg} mice was performed. Sixteen hours after injection of 20 to 25×10^6 CLL cells, significantly less *Rhoh*$^{-/-}$ CLL cells compared with *WT* CLL cells were detected in the BM (3×10^{-3} % ± 0.17 vs 1.7×10^{-3} % ± 0.23; WT vs *Rhoh*$^{-/-}$, mean ± SEM, respectively, MWU test, $P = .004$; Figure 1A). Despite an increased spontaneous apoptosis rate (supplemental Figure 1, available on the *Blood* Web site; see the Supplemental Materials link at the top of the online article), the number of *Rhoh*$^{-/-}$ CLL cells remaining in the PB was slightly increased (Figure 1B), suggesting impaired trafficking of *Rhoh*$^{-/-}$ CLL cells in vivo. This explanation was further supported by the observation that 4 weeks after transplantation of 2×10^7 CLL cells intraperitoneally, disease burden in the blood in recipient mice was significantly reduced in the absence of RhoH (13.1 ± 3 K/μL vs 1.2 ± 0.3 K/μL; WT vs *Rhoh*$^{-/-}$, respectively, $P = .004$; Figure 1C), and survival was significantly prolonged as assessed by χ^2 test ($P = .014$; Figure 1D) and Kaplan-Meier analysis (supplemental Figure 2). This was associated with lower BM infiltration and spleen weights in surviving animals receiving *Rhoh*$^{-/-}$ CLL compared with *WT* CLL cells (data not shown). To further address early engraftment kinetics a separate group of animals was killed 3 weeks after transplantation. At that time recipient mice transplanted with *Rhoh*$^{-/-}$ CLL cells also had significantly less CLL cells in the PB (3.49 ± 0.86 K/μL vs 0.87 ± 0.2 K/μL; WT vs *Rhoh*$^{-/-}$, respectively, $P = .01$; Figure 1E). In addition, the infiltration of CLL cells in the BM was significantly reduced in the absence of RhoH ($30.2 \pm 28.6 \times 10^8$ vs $0.58 \pm 0.1 \times 10^8$ CLL cells; WT vs *Rhoh*$^{-/-}$, respectively, $P = .025$; Figure 1F-G) and spleen weights were significantly lower in mice receiving *Rhoh*$^{-/-}$ CLL cells (362.5 ± 138.8 mg vs 131.3 ± 6.3 mg, WT vs *Rhoh*$^{-/-}$, respectively, $P = .006$; Figure 1H).

Impaired contact-dependent interaction of *Rhoh*$^{-/-}$ CLL cells and NLCs in vitro and pseudofollicle formation in *Rhoh*$^{-/-}$ spleens in vivo

In CLL patients, leukemic cells are organized into pseudofollicles within the BM and SLTs.[3,5] Long-term in vitro culture of PBMNCs from CLL patients gives rise to $CD68^+$ monocyte-derived adherent

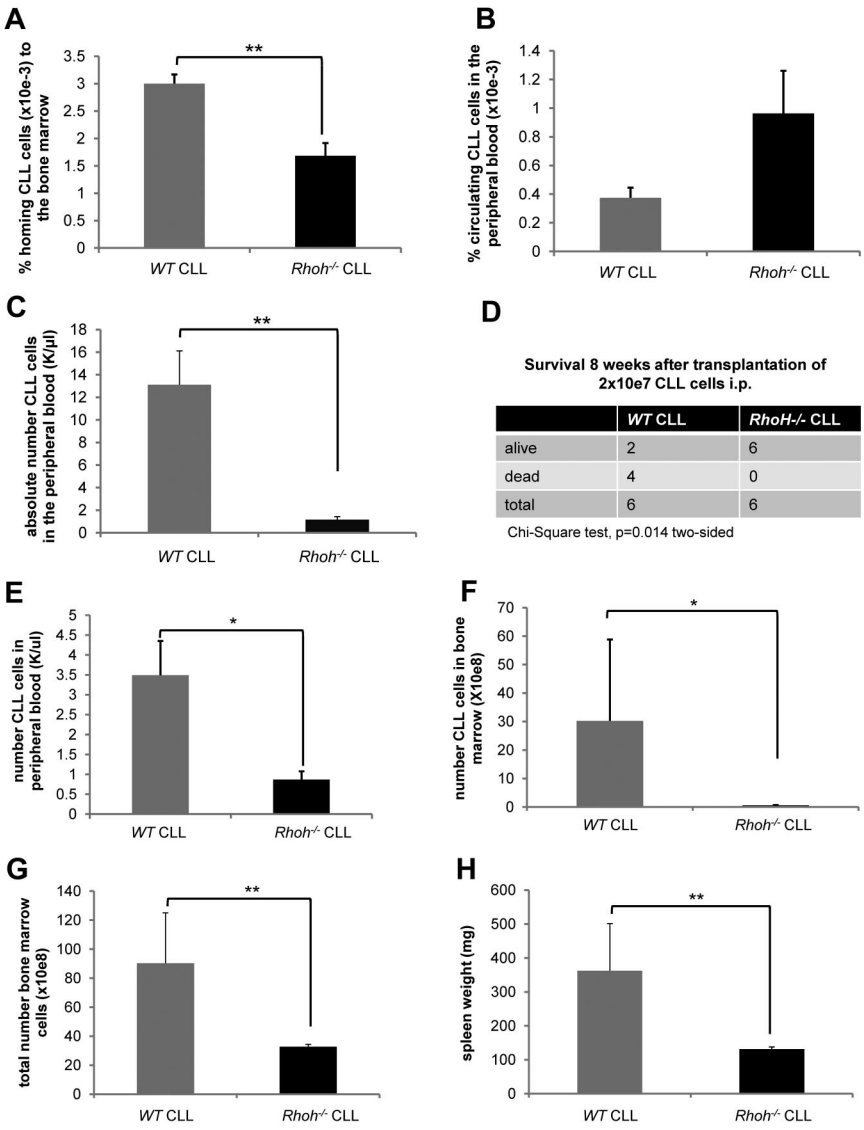

Figure 1. Reduced BM homing of *Eμ-TCL1*^{Tg};*Rhoh*$^{-/-}$ CLL cells. (A) The number of CD3$^-$/CD5$^+$/IgM$^+$CLL cells was determined by flow cytometry and the ratio of CLL cells detected in the BM to number of injected CLL cells was calculated. (B) The ratio of CLL cells detected in the PB to number of injected CLL cells was calculated. (A-B) Data show mean ± SEM of CLL cells homing to the BM and circulating in the PB 16 hours after injection of 20 to 25 × 10^6 CLL cells (*WT* versus *Rhoh*$^{-/-}$, mean ± SEM, $^{**}P = .004$ and $P = .2$, Mann-Whitney *U* (MWU) test, n = 6 recipients). (C) The number of CD3$^-$/CD5$^+$ CLL cells was determined in the PB of recipients by flow cytometry. Data show mean ± SEM of CLL cells circulating in the PB 4 weeks after transplantation of 2 × 10^7 CLL cells (*WT* versus *Rhoh*$^{-/-}$, mean ± SEM, $^{**}P = .004$, MWU test, n = 6 recipients/group). (D) Comparison of survival of *Rag2*$^{-/-}$*/IL2*$\gamma^{-/-}$ recipients 8 weeks after transplantation. (E) Data show mean ± SEM of CD3$^-$/CD5$^+$ CLL cells circulating in the PB 3 weeks after transplantation as assessed by flow cytometry (*WT* versus *Rhoh*$^{-/-}$, mean ± SEM, $^*P < .05$, MWU test, n = 6 recipients/group). (F) Bars indicate mean ± SEM of total BM cells 3 weeks after transplantation (*WT* versus *Rhoh*$^{-/-}$, mean ± SEM, $^*P < .05$, MWU test, n = 6 recipients/group) and (G) CLL cells present in the BM (*WT* versus *Rhoh*$^{-/-}$, mean ± SEM, $^*P < .05$, MWU test, n = 6 recipients/group). (H) Data show mean ± SEM of spleen weights in recipients 3 weeks after transplantation (*WT* versus *Rhoh*$^{-/-}$, mean ± SEM, $^*P < .05$, MWU test, n = 6 recipients/group).

NLCs that produce chemokines, such as CXCL12 and CXCL13, and support CLL cell survival.[5-7] It has been shown that these cells also exist in lymph nodes of CLL patients.[5] The generation of murine NLCs and their interaction with CLL cells in vitro was next examined. In vitro culture of MNCs from the spleen (Figure 2A) and PBMNCs (Figure 2B) of *Eμ-TCL1*^{Tg};*Rhoh*$^{-/-}$ and *Eμ-TCL1*^{Tg};*WT* mice resulted in outgrowth of adherent cells that appeared morphologically similar to NLCs and expressed CD68 (supplemental Figure 3A-B). In age/disease-stage matched animals the number of *Rhoh*$^{-/-}$ CLL cells (Figure 2A-B arrows) associated with either splenic (7 ± 1.7 vs 17 ± 1.3; *Rhoh*$^{-/-}$ vs *WT*, mean ± SEM, $P = .0001$; Figure 2A) or PBMNC-derived (2 ± 0.3 vs 16 ± 3; *Rhoh*$^{-/-}$ vs *WT*, $P = .001$; Figure 2B) *Rhoh*$^{-/-}$ NLCs was significantly reduced as enumerated in randomly selected microscopic fields in 2 to 4 independent experiments. The input CLL cell numbers were lower in in vitro cultured PBMNC samples because of lower leukemic burden in the PB of age-matched mice, which could contribute to the lower number of CLL cells associated with NLCs. However, in the spleen samples obtained from mice older than 8 months, the percentage of CLL cells were similar in *WT* and *Rhoh*$^{-/-}$ samples and accordingly the number of CLL cells plated was comparable. Despite equivalent CLL cell input, the number of CLL cells interacting with NLCs was still significantly decreased.

To better assess CLL-microenvironment interactions in vivo, spleen sections of *Eμ-TCL1*^{Tg};*Rhoh*$^{-/-}$ and *Eμ-TCL1*^{Tg};*WT* mice were examined for macrophage galactose-specific lectin 2 (Mac-2)$^+$ cells within pseudofollicles (supplemental Figure 4A). Mac-2 expressing myeloid-lineage cells, including macrophages and dendritic cells, have been shown to produce the B-cell attracting chemokine CXCL13, thus regulating B cell positioning within lymphoid organs.[7,23,24] The percentage of Mac-2$^+$ cells morphologically distinguishable as macrophages and dendritic cells was significantly increased in *Eμ- TCL1*^{Tg};*Rhoh*$^{-/-}$ spleens (46.7 ± 3.6/section vs 20.8 ± 1.2; *Rhoh*$^{-/-}$ vs *WT*, mean ± SEM, $P = .004$), and pseudofollicles (34.8 ± 7.7/chosen area vs 16.7 ± 3.4; *Rhoh*$^{-/-}$ vs *WT*; $P = .05$; supplemental Figure 4B). Therefore the ratio of *Rhoh*$^{-/-}$ CLL cells to accessory cells was also reduced in situ in *Rhoh*$^{-/-}$ spleens. As previously described, splenic *Rhoh*$^{-/-}$ CLL cells also demonstrate an increased apoptosis rate.[20] These data suggest that *Rhoh*$^{-/-}$ CLL cells lack survival signals from the microenvironment because of impaired access/interaction despite a

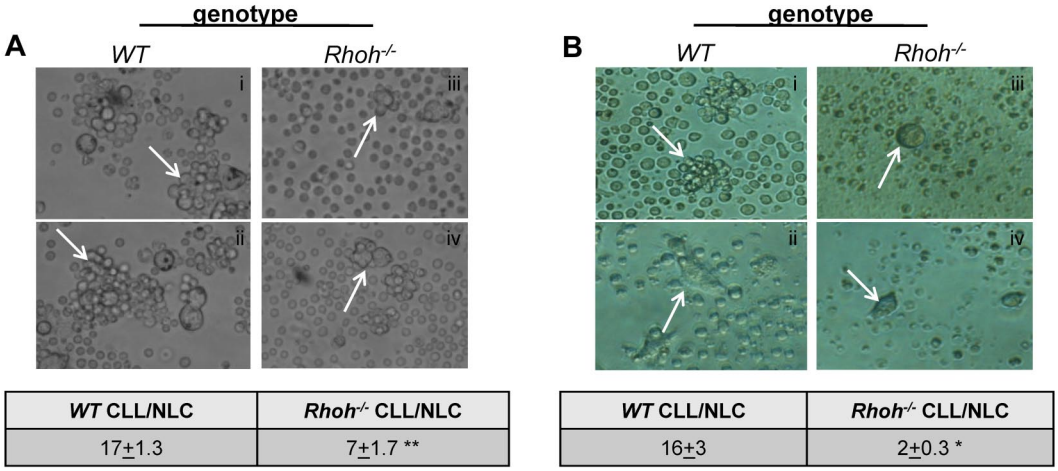

WT CLL/NLC	*Rhoh*$^{-/-}$ CLL/NLC
17±1.3	7±1.7 **

WT CLL/NLC	*Rhoh*$^{-/-}$ CLL/NLC
16±3	2±0.3 *

Figure 2. Impaired cell-cell contact of *Eμ-TCL1*^{Tg};*Rhoh*$^{-/-}$CLL and NLCs. (A-B) show colocalization of murine NLCs with CLL cells (arrowheads) in representative bright-field photomicrographs of *WT* and *Rhoh*$^{-/-}$ (A) spleen cells and (B) PBMNCs of *Eμ-TCL1*^{Tg} animals at 200× magnification (n = 2-4). The table for each panel indicates number of CLL cells colocalized per NLC enumerated in 2 randomly selected microscopic fields at 200× magnification (*WT* versus *Rhoh*$^{-/-}$; mean ± SEM, $^{**}P = .0001$ and $^{*}P = .001$, Student *t* test).

potential compensatory increase in chemokine-expressing cells within the spleen and exhibit a potentially altered cell-intrinsic response to chemokine signaling pathways.

Impaired directed migration of *Rhoh*$^{-/-}$ CLL cells toward CXCL12 and CXCL13 in vitro

Migration and homing of leukemic cells to specific supportive cell environments has been postulated to support leukemia cell survival and disease progression.[25-27] The chemokines CXCL12 and CXCL13 are known to regulate normal B lymphocyte trafficking, positioning within lymphoid follicles, and homing to the BM.[28,29] Directed migration of *Eμ-TCL1*^{Tg};*WT* and *Eμ-TCL1*^{Tg};*Rhoh*$^{-/-}$ CLL cells in vitro in response to these chemokines was next examined. Input and migrated splenocyte fraction of B cells were identified as B220^{+} and CLL cells as CD3^{-}/CD5^{+}/IgM^{+} using flow cytometric analysis. Directed migration of *Eμ-TCL1*^{Tg};*Rhoh*$^{-/-}$ CLL cells toward CXCL12 was significantly reduced compared with *Eμ-TCL1*^{Tg};*WT* CLL cells (1.7% ± 0.3 vs 7.3% ± 0.4; *Eμ-TCL1*^{Tg};*Rhoh*$^{-/-}$ vs *Eμ-TCL1*^{Tg};*WT*, $P < .001$; Figure 3A). ICAM-1 is a known ligand for LFA-1 and facilitates transmigration of lymphocytes across endothelial barriers.[30] Despite increased overall response in the presence of ICAM-1 fewer *Rhoh*$^{-/-}$ CLL cells migrated toward CXCL12 (19.4% ± 5 vs 44.6% ± 1.6;

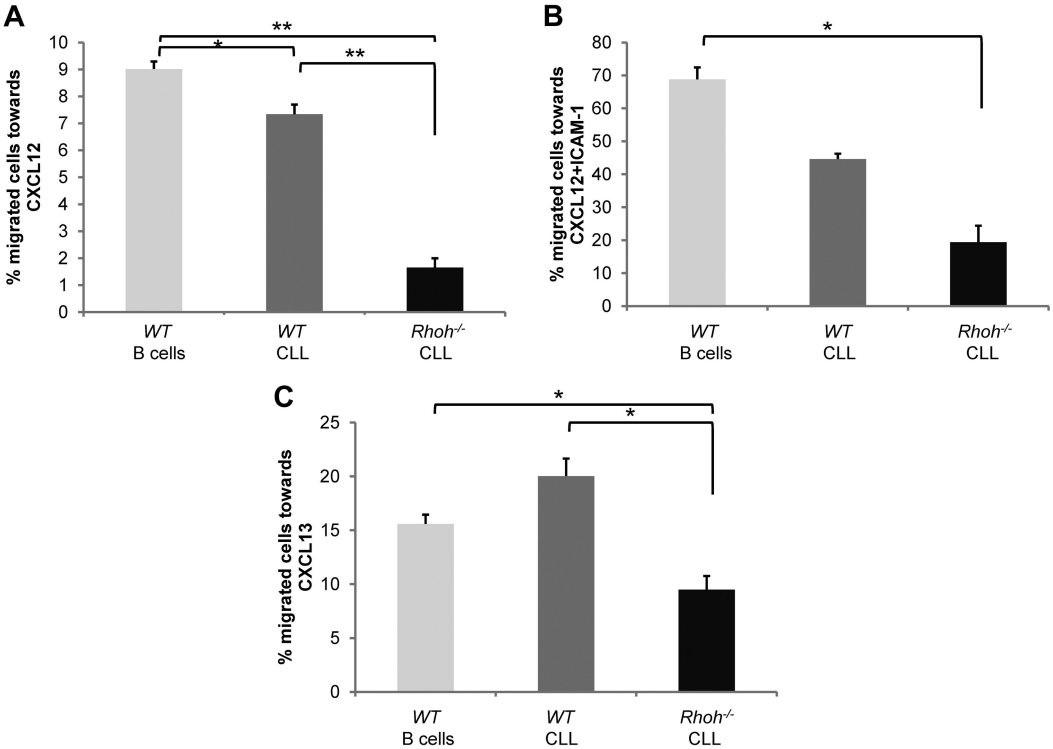

Figure 3. Significantly impaired CXCL12 and CXCL13-directed migration of *Eμ-TCL1*^{Tg};*Rhoh*$^{-/-}$CLL cells. Percent migration of B220^{+} B cells or CD3^{-}/CD5^{+}/IgM^{+}CLL cells after 4 hours in response to (A-B) CXCL12 and (C) CXCL13 in the absence (A-C) or presence (B) of 40 ug/mL ICAM-1. Shown is 1 representative experiment of 2 giving similar results. Data show mean ± SEM of triplicate wells (*WT* versus *Rhoh*$^{-/-}$; $^{*}P < .05$ and $^{**}P < .005$, Student *t* test, n = 3).

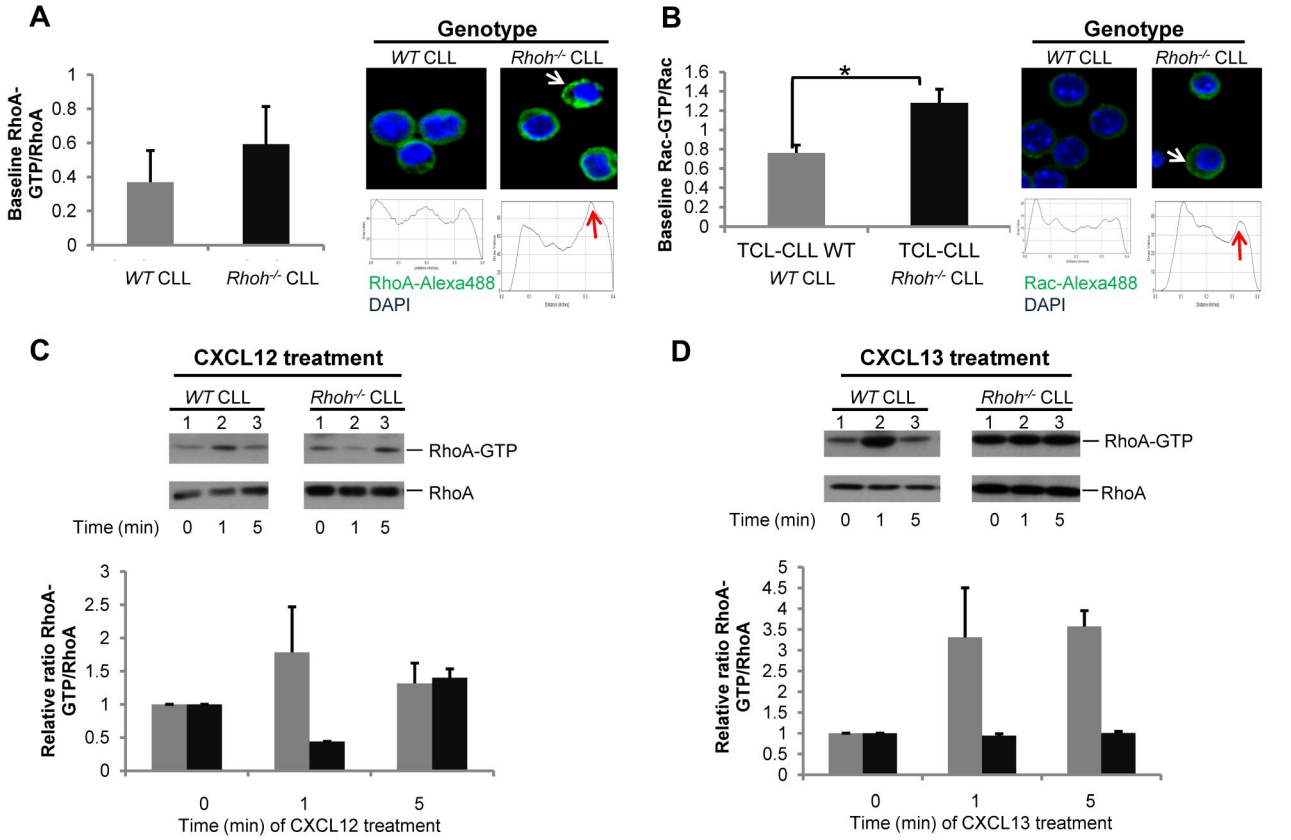

Figure 4. Increased RhoA and Rac activity and dyregulated RhoA activation after stimulation with CXCL12 and CXCL13 in *Eμ-TCL1*^{Tg};*Rhoh*$^{-/-}$CLL cells. (A) RhoA and (B) Rac activity determined by pull-down assays in *WT* versus *Rhoh*$^{-/-}$CLL samples (*WT* versus *Rhoh*$^{-/-}$CLL; mean ± SEM, **P* < .05, Student *t* test, n = 3). Representative photomicrographs showing immunofluorescence staining and membrane localization of (A) RhoA (green), (B) Rac (green), and DAPI stained nuclei (blue) in fixed *WT* and *Rhoh*$^{-/-}$CLL cells. Representative dot plot analysis of RhoA and Rac distribution randomly selected from 3 to 4 microscopic fields at 600× magnification are exhibited and show increased membrane localization as indicated by arrowheads in *Rhoh*$^{-/-}$cells. Primary *WT* and *Rhoh*$^{-/-}$CLL cells were analyzed for activated and total RhoA protein after (C) CXCL12 and (D) CXCL13 stimulation. Top panels: activated (GTP-bound) RhoA; bottom panels: total RhoA protein. Bar graphs depict the relative ratio of GTP-bound to total protein obtained by densitometric measurement of the respective bands in blots of 2 independent experiments. These ratios were normalized to the unstimulated condition and indicate the fold increase after chemokine stimulation (gray bars: *WT*CLL vs black bars: *Rhoh*$^{-/-}$CLL; mean ± SEM).

Eμ-TCL1^{Tg};*Rhoh*$^{-/-}$ vs *Eμ-TCL1*^{Tg}, *P* = .02; Figure 3B). The number of *Eμ-TCL1*^{Tg};*Rhoh*$^{-/-}$ CLL cells attracted by CXCL13 was also significantly decreased (9.5% ± 1.3 vs 20.0% ± 1.6, *Eμ-TCL1*^{Tg};*Rhoh*$^{-/-}$ vs *Eμ-TCL1*^{Tg};*WT*, *P* < .01; Figure 3C). Additional in vitro studies examining migration at 2 hours and 6 hours revealed that this defect was not simply because of delayed migration (data not shown). The impaired migration was moreover not because of decreased expression of the cognate receptors CXCR4 and CXCR5 as determined by flow cytometry. CXCR4 expression was significantly increased on *Rhoh*$^{-/-}$ CLL cells (MFI 169 ± 6 vs 137 ± 5; *Eμ-TCL1*^{Tg};*Rhoh*$^{-/-}$ vs *Eμ-TCL1*^{Tg};*WT*, *P* < .01; supplemental Figures 5A and 6A), whereas CXCR5 expression was only modestly decreased compared with *WT* CLL cells (MFI 5770 ± 1290 vs 7392 ± 1613; *Eμ-TCL1*^{Tg};*Rhoh*$^{-/-}$ vs *Eμ-TCL1*^{Tg};*WT*, *P* = .45; supplemental Figures 5C and 6B). The difference in CXCR5 receptor expression may be physiologically relevant because serum levels of CXCL13 but not CXCL12 were considerably increased in *Rhoh*$^{-/-}$ mice (supplemental Figure 5B-D) suggesting a compensatory response in vivo, which is also consistent with the increased percentage of Mac-2^{+} cells detected in *Eμ-TCL1*^{Tg};*Rhoh*$^{-/-}$ spleens. Homing of lymphocytes in vivo is affected by transient, and then firm adhesion that is mediated by integrins. Adhesion to fibronectin a known β1 integrin ligand was significantly increased in the presence of CXCL12 in *Rhoh*$^{-/-}$ CLL (75.7 ± 6.3% vs 44.7 ± 3.9, *Rhoh*$^{-/-}$ vs *WT*, *P* = .02; supplemental Figure 5E-F), whereas adhesion to β2 integrins, such as ICAM-1, was not affected (data not shown). This may reflect increased expression of CXCR4 in the absence of RhoH or could suggest that RhoH is involved in regulation of chemokine induced inside-out signaling in CLL cells. These results demonstrate that RhoH is required for directed CLL cell migration in response to chemokines implicated in B-cell trafficking in vivo. Increased adhesion in the presence of chemokine stimulation may further contribute to dysfunctional transendothelial migration of *Rhoh*$^{-/-}$ CLL cells in vivo.

Dysregulated activity of RhoA and Rac in *Rhoh*$^{-/-}$ CLL

We next determined whether these defects in *Rhoh*$^{-/-}$ CLL cytoskeletal functions were mediated by alterations in Rho GTPase signaling pathways. Rho GTPases, particularly RhoA and Rac, are major regulators of cell shape and migration.[9,31] These functions require localized activation of Rho GTPases at the cell membrane in response to chemokine stimulation.[32] Deficiency of RhoH was previously shown to be associated with increased basal Rac activity and abnormal chemokinesis in hematopoietic cells.[10,33] In *Eμ-TCL1*^{Tg};*Rhoh*$^{-/-}$ CLL cells total RhoA protein expression was rather increased and total Rac protein expression rather decreased when normalized to β-actin. However, *Eμ-TCL1*^{Tg};*Rhoh*$^{-/-}$ CLL cells showed increased baseline activation and membrane localization of RhoA (Figure 4A) and Rac (Figure 4B) as determined in effector pull-down assays. After stimulation with CXCL12 and CXCL13 there was no further activation of RhoA (Figure 4C-D) or Rac (supplemental Figure 7A-B) in response to either cytokine in

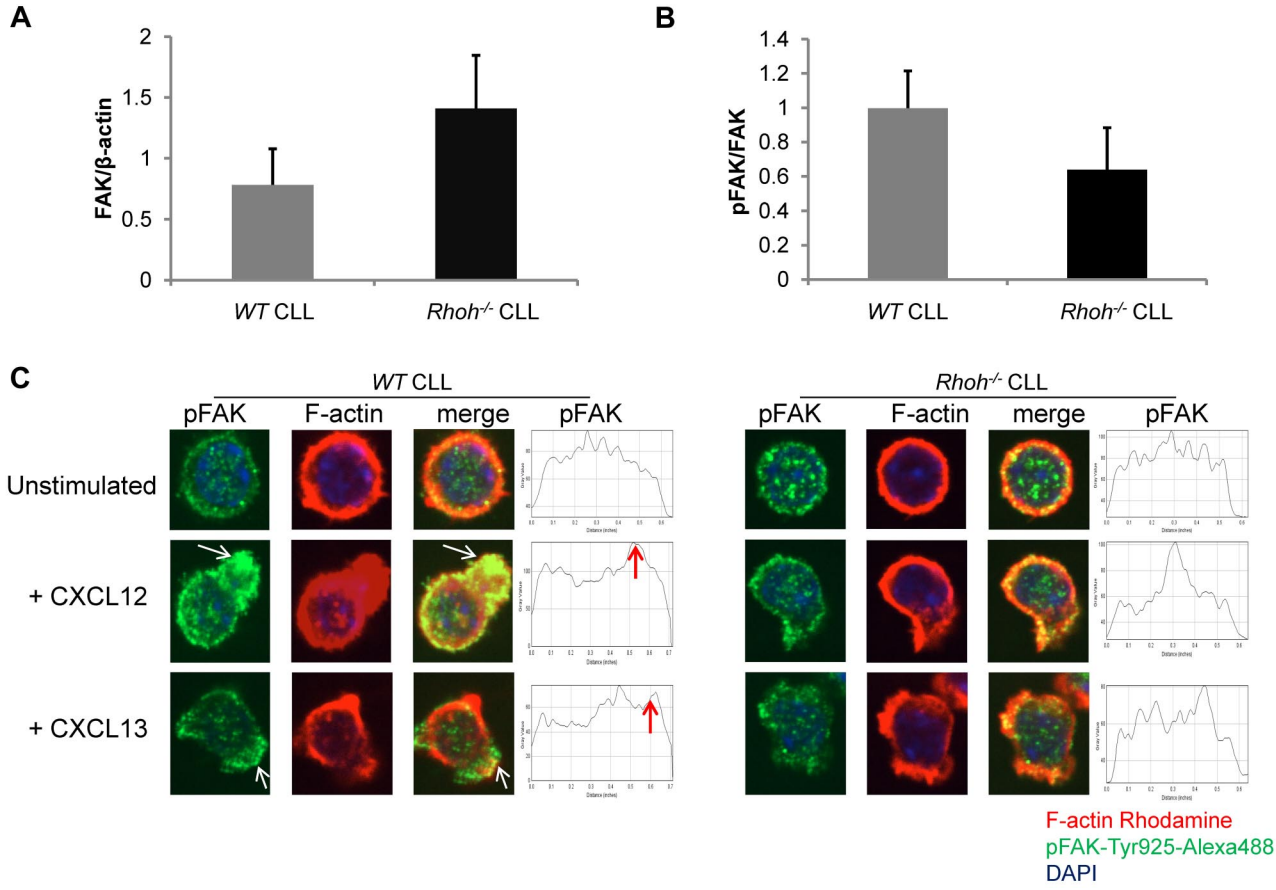

Figure 5. Impaired and less polarized recruitment of phospho-FAK-Tyr925 to membrane ruffles in *Eμ-TCL1*^{Tg};*Rhoh*$^{-/-}$CLL cells after chemokine stimulation. (A) Total FAK and (B) phospho-FAK expression determined by immunoblot in *WT* versus *Rhoh*$^{-/-}$CLL samples (*WT* versus *Rhoh*$^{-/-}$CLL; mean ± SEM, n = 3). (C) Primary murine CLL cells were stained for pFAK-Tyr925 (green), F-actin (rhodamine-phalloidin, red), and nuclear DAPI (blue). Merged confocal photomicrographs are also shown, all 600× magnification. On the right representative dot plots of pFAK-Tyr925 distribution pattern in CLL cells selected from 3 to 4 microscopic fields at 600× magnification. Arrowheads indicate accumulation of pFAK-Tyr925 in a polarized fashion in CXCL12 or CXCL13 stimulated *WT*CLL cells (representative of 2 independent experiments).

the absence of RhoH. Thus, RhoH appears critical for the regulation of RhoA and Rac activity in CLL cells.

Impaired chemokine-induced activation and recruitment of focal adhesion kinase to membrane ruffles in *Rhoh*$^{-/-}$ CLL

FAK is activated by phosphorylation via Src kinases and regulates adhesion and directed cell migration in an agonist-specific fashion.[34] Activation of FAK regulates RhoA and Rac activity via guanine nucleotide exchange factors (GEFs) and GTPase activating proteins (GAPs) in a spatiotemporal fashion.[11] Baseline expression and phosphorylation of FAK was not significantly altered in *Rhoh*$^{-/-}$ CLL (Figure 5A-B). However, after activation with CXCL12 and CXCL13 accumulation of tyrosine-925 phosphorylated FAK (pFAK-Tyr925) appeared impaired and was less polarized within membrane ruffles in *Rhoh*$^{-/-}$ CLL cells (Figure 5C). This may suggest that RhoH plays a role in Scr-induced FAK phosphorylation and its localization. To assess the localization of RhoH in relation to auto and src-phosphorylated-FAK in B lymphoid cells, *RHOH-EGFP* was introduced into the precursor B-cell leukemia line Nalm-6 (supplemental Figure 8A-C). After stimulation with CXCL12, RhoH and pFAK-Tyr925 colocalized in membrane ruffles and appeared in close vicinity at sites of cell-cell contact (supplemental Figure 8B-C). Thus, altered pFAK localization in *Rhoh*$^{-/-}$ CLL cells was associated with defective regulation of GTPase activation and impaired directional movement and may contribute to the defective cell-cell contact with NLCs in vitro.

Reduced RhoH expression and dysregulated RhoA/Rac activity after lenalidomide treatment of primary human CLL cells

Immunomodulatory drugs, such as lenalidomide, have recently shown efficacy in CLL, although the mechanism of action remains obscure.[35-37] Given its influence on Rho GTPase activity in hematopoietic cells that was similar to differences noted above,[38] we next treated primary human CLL samples in vitro with 0.5μM lenalidomide, a concentration achieved in patients in vivo with daily administration of 2.5-5 mg lenalidomide, or vehicle and assessed GTPase activity. In 4 of 5 CLL samples, lenalidomide treatment resulted in decreased RhoH expression (Figure 6A) and increased RhoA and Rac activation (Figure 6B-C). Given the in vitro effect, we next investigated whether in vivo treatment with lenalidomide would result in altered GTPase expression and activity in 6 paired CLL patient samples. GTPase expression and activity was assessed in CLL samples obtained from relapsed patients before (pre) and after 8 days (d8) of in vivo treatment with 2.5 to 5 mg/d of lenalidomide. Compared with pretreated samples, there was a significant decrease in RhoH expression (0.44 ± 0.11 vs 0.29 ± 0.09; pre vs d8, mean ± SEM, n = 6 patients, $P = .004$; Figure 7A) and increase in RhoA (0.08 ± 0.02 vs 0.40 ± 0.05; pre vs d8, $P = .002$; Figure 7B) and Rac (0.77 ± 0.08 vs 1.43 ± 0.36; pre vs d8, $P = .002$; Figure 7C) activity after in vivo lenalidomide treatment. Similar to murine *Rhoh*$^{-/-}$ CLL cells, pFAK-Tyr925 staining appeared less pronounced within membrane ruffles and at

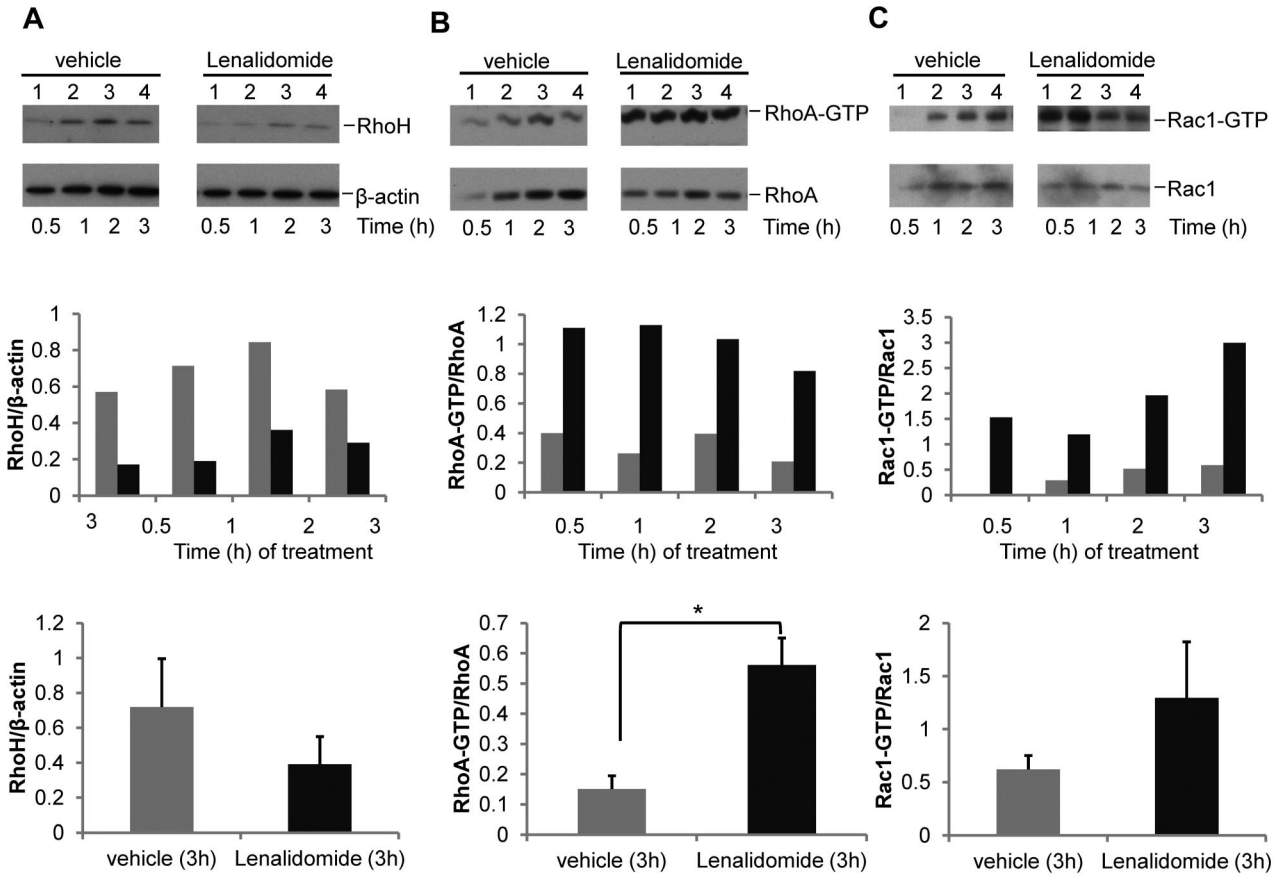

Figure 6. In vitro lenalidomide treatment of primary human CLL cells results in decreased RhoH expression and increased RhoA and Rac activation. Primary human CD19$^+$CLL samples were treated with vehicle or 0.5μM lenalidomide for the indicated time points. CLL content was ≥ 90% in all cases. One representative experiment of 5 is shown. (A) Western blot analysis for RhoH protein expression. (B-C) RhoA and Rac activities determined by pull-down assays. In each panel the protein of interest or active (GTP-bound) protein is shown in top panel and the loading control or total protein is shown in the bottom panel. The bar graphs in the middle panel show ratio of RhoH to β-actin and activated GTP-bound RhoA or Rac protein to total RhoA or Rac protein based on densitometric measurements of the respective Western blot bands. The bar graphs in the bottom panel summarize the respective ratios obtained in all 5 patients (gray bars: vehicle versus black bars: lenalidomide treatment; mean ± SEM; (A) $P = .09$; (B) $^*P = .002$; (C) $P = .24$, Student t test, n = 5).

sites of cell-cell contact (data not shown). Despite a low overall migratory response of CLL cells after cryopreservation, chemokine-induced in vitro migration tended to be reduced in lenalidomide-treated patient samples (15%-40% vs 100%, d8 vs pre and 32%-89% vs 100%, d8 vs pre toward CXCL13 and CXCL12, respectively; data not shown). Overall, these data show that lenalidomide-treatment of CLL in vitro and in vivo closely resemble the findings in the *Eμ-TCL1*^{Tg} animal model in the absence of RhoH and suggest a previously unrecognized mechanism for lenalidomide microenvironment effects in CLL.

Discussion

RhoH was first identified as a fusion transcript with Bcl-6 in B-cell diffuse large cell lymphoma[12] and subsequently implicated in other B-cell malignancies.[13-15] Despite significant progress in the understanding of RhoH function in the TCR signaling pathway where it facilitates colocalization of ZAP70 and LCK to the immune synapse,[16,18,19] the role of RhoH in B-cell malignancies is still obscure and *Rhoh*$^{-/-}$ mice have a relatively modest B cell phenotype. RhoH has no intrinsic GTPase activity and remains in a GTP-bound and constitutively active state. Therefore it is regulated by expression levels and posttranslational modifications.[12] The expression of *RHOH* correlates with *ZAP70* expression in human primary CLL cells suggesting an association of increased *RHOH* expression with high-risk features.[39] We have previously demonstrated that disease progression in a murine model of CLL is attenuated in the absence of RhoH despite a significant T-cell immunodeficiency[20] without fully clarifying the mechanism. Here we explored the potential effect of RhoH deficiency on migration and the interaction of CLL cells with supporting cells of the malignant microenvironment.

It has become increasingly clear that a fraction of CLL cells can proliferate in vivo within supportive niches and that response to chemokines and access to tissue microenvironment are important factors contributing to their survival and proliferation.[3,6,7] Our data indicate that *Rhoh*$^{-/-}$ CLL cells are able to home to the BM in vivo less efficiently than *WT* CLL cells and exhibit decreased directed migration in vitro in response to the chemokines CXCL12 and CXCL13. CXCL12 regulates homing of CLL cells to the BM environment via functional CXCR4 receptor expressed on these cells and confers contact-dependent protection from spontaneous and chemotherapy-induced apoptosis within pseudofollicles.[6,40] It has been shown that CXCR4 inhibition in vitro blocks CXCL12 induced activation, migration, and signaling, and partially sensitizes CLL cells to apoptosis.[41] In accordance to normal B cells, CLL cells recirculate and home to the BM, where they receive survival and proliferation signals from NLCs or stromal cells in a cell-contact dependent manner.[25,28,42] This may well contribute to

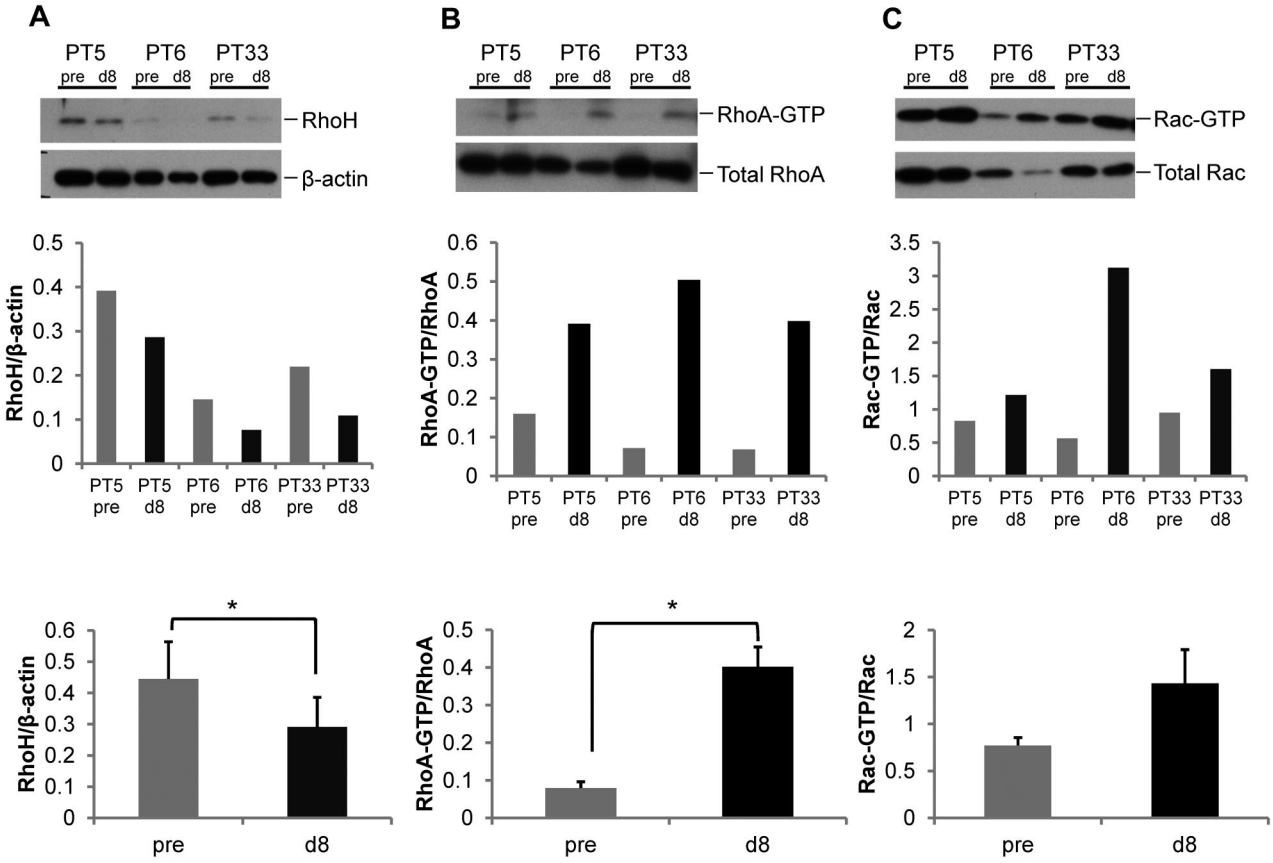

Figure 7. In vivo lenalidomide treatment of primary human CLL cells results in decreased RhoH expression and increased RhoA and Rac activation. CLL patients were treated daily for 8 days with 2.5 mg lenalidomide within a clinical phase 1 study. All samples obtained from 6 patients before (pre) and on day 8 (d8) of lenalidomide treatment contained $>$ 87% $CD19^+$ cells. Representative blots of 3 patients are displayed. (A) Western blot analysis for RhoH protein expression. (B-C) RhoA and Rac activities determined by pull-down assays. In each panel the protein of interest or active (GTP-bound) protein is shown in top panel and the loading control or total protein is shown in the bottom panel. The bar graphs in the middle panel show ratio of RhoH to β-actin and activated GTP-bound RhoA or Rac protein to total RhoA or Rac protein based on densitometric measurements of the respective Western blot band before and after treatment for each of the 3 patients. The bar graphs in the bottom panel summarize the ratios obtained in all 6 patients (gray bars: pre treatment vs black bars: day 8 results; mean ± SEM, $^*P < .05$, Student *t* test, n = 6).

their sustained survival and relative resistance to standard chemotherapy. Of note it has been demonstrated that hematopoietic cell-specific Lyn substrate-1 (HS1)–deficient CLL cells that home preferentially to the BM result in a more aggressive disease phenotype in *Eμ-TCL1*^{Tg}*;HS1*$^{-/-}$ mice, further underlining the importance of microenvironment cross-talk in CLL progression.[26] Stromal cells in B cell areas of SLT secrete CXCL13, which regulates lymphocyte homing to these tissues and positioning of circulating naive B cells within follicles via the cognate receptor CXCR5.[29] We show here that RhoH regulates CLL migration in response to these chemokines and the resulting defect in the CLL microenvironment interaction probably reduces this contact-dependent protection from spontaneous apoptosis within proliferation centers. Impaired access to the supportive microenvironment in the absence of RhoH may therefore contribute to the increased apoptosis rate detected in *Rhoh*$^{-/-}$ CLL cells from the PB and spleens. Interestingly, this phenotype appears to be specific for the malignant CLL cells as it was previously demonstrated that RhoH deficiency had no impact on in vitro migration of normal B cells.[20]

Compared with *Eμ-TCL1*^{Tg}*;WT* mice the percentage of cells staining positive for Mac-2, a well-established marker for staining murine macrophages and dendritic cells, was increased in *Rhoh*$^{-/-}$ spleens. Although an increased number of tumor-associated macrophages so far has been associated with a poor prognosis in most clinical cancer studies,[43] there is also evidence that activated macrophages can exhibit a tumoricidal effect in CLL.[44] In addition, it has been demonstrated that both dendritic cells and macrophages produce the B-cell attracting chemokine CXCL13,[23] and that chemokines as well as cell-contact–dependent interaction with the NLCs supports CLL cell survival.[5,7] We demonstrate reduced interaction of murine CLL cells with NLCs derived from the PB and spleen of *Eμ-TCL1*^{Tg}*;Rhoh*$^{-/-}$ mice.

Rho GTPases regulate cell shape and migration via complex interactions with severaleffector pathways that control actin polymerization, focal adhesion complexes, and kinase activation.[9,11,31] The Rho GTPase Rap1 has been implicated in activation of integrins resulting in defective transendothelial migration and recirculation of CLL cells.[45] RhoH was previously demonstrated by us and others to antagonize Rac signaling[10,22,33,46] and was also implicated in maintenance of LFA-1 in the nonactivated state.[47] Interestingly, it has also been shown that CLL cells can home to the spleen in a LFA-1 and VLA4-independent manner, thus LFA-1 expression and VLA-4 activation appeared critical for the ability of these cells to transmigrate through endothelial barriers and home to SLTs and the BM.[27] Here we demonstrate that RhoH deficiency leads to increased basal activation and dysregulated responses to chemokine stimulation of both RhoA and Rac. Localized activation of Rac and RhoA at opposite ends of the migrating cell probably depends on cross-talk between these GTPases and their antagonistic regulation. It has been demonstrated that active Rac can both suppress and increase RhoA activation and vice versa.[48-51] In this respect Src family kinases and the protein tyrosine kinase FAK can

serve as critical coordinators of the cytoskeleton response as they are able to interact with both GEFs and GAPs thus regulating Rac and RhoA GTPase activity.[11,52] We found that the Src-dependent phosphorylated form of FAK colocalizes with RhoH in membrane ruffles and is located in close vicinity to RhoH at sites of cell-cell contact. Despite overall normal expression and activation levels, pFAK-Tyr925 staining also appeared less polarized and with lower accumulation in membrane ruffles in CLL cells that lack RhoH. This may explain the defective migration of CLL cells lacking RhoH, because both RhoA and Rac are required for coordinated cell migration in many hematopoietic cells and our data suggest that RhoH may contribute to the regulation and modulation of both their activity and localization.

Importantly, we also demonstrate that the finding of diminished RhoH expression might have relevance to lenalidomide, an immune modulatory agent with diverse mechanisms of action in CLL including B-cell activation and stromal cell interactions.[53] Although the mechanism of B-cell activation of CLL through CD154 induction was recently reported by us, little understanding of how lenalidomide inhibits stromal interaction has been put forward.[54] Herein we demonstrate that both ex vivo and in vivo treatment of human CLL cells with the immunomodulatory drug lenalidomide results in reduced RhoH expression and similar dysregulation of RhoA and Rac activation and a slightly altered distribution pattern of pFAK within CLL cells after chemokine stimulation. Furthermore, additional data suggest that these molecular changes after in vivo treatment with low doses (2.5 mg) of lenalidomide are also associated with reduced migratory potential of CLL cells in response to chemokines in vitro. In CLL this finding of pharmacodynamic effect of RhoH modulation at very low doses of lenalidomide (2.5 mg) is important because of the poor tolerance of this agent in CLL at higher doses (25 mg) used in lymphoma and multiple myeloma.[55] The microenvironmental influence on CLL cell protection from apoptosis from cytotoxic agents is well described.[56] These findings suggest that lenalidomide at low doses might have the potential to augment efficacy of standard cytotoxic therapies used in CLL whose activity is blunted in compartments, such as the BM. However, future work focusing on how decreased RhoH expression influences CLL cell migration in response to chemokines in more detail and the exact mechanism of how lenalidomide down-regulates RhoH in CLL remains unknown and is under investigation at this time.

Taken together, our findings provide novel mechanistic insights in the effects of lenalidomide treatment in CLL patients and demonstrate that RhoH is a critical component downstream of chemokine receptor signaling required for colocalization and cell-contact–dependent interaction of CLL cells with supportive microenvironment tissue in vivo. This is of clinical relevance as interference with both of these aspects in CLL pathogenesis seems promising for the development of novel and complementary treatment strategies for this common, yet incurable disease.

Acknowledgments

The authors acknowledge the technical advice, helpful discussions, and comments from Dr Abel Sanchez-Aguilera and other members of the Williams and Armstrong laboratories, and are grateful for expert animal husbandry and support from Meaghan McGuinness, Chad Harris and Megan Bariteau. They also thank the Rodent Histopathology and Specialized Histopathology Services from the Longwood Core of the Dana-Farber/Harvard Cancer Center and particularly Scott Rodig for technical support.

This work was supported by grants from the National Institutes of Health (CA113969 to D.A.W.; P50-CA140158 to A.J.J. and J.C.B.; P01 CA95426 to J.C.B.; and K12 CA133250 to A.J.J. and J.C.B.), the Deutsche Forschungsgemeinschaft TR 1005/1-1 (A.T.), and The D. Warren Brown Foundation (J.C.B.).

Authorship

Contribution: A.T. and D.A.W. designed research; A.T., A.J.J., and J.W. performed research; A.T. and D.A.W. analyzed and interpreted data; A.J.J., W.G.B., L.A.A., and J.C.B. contributed vital new reagents and provided scientific advice related to the human CLL experiments and lenalidomide work; A.T. and D.A.W. wrote the paper; and all the authors reviewed versions of the paper and approved of the final version.

Conflict-of-interest disclosure: The authors declare no competing financial interests.

Correspondence: David A. Williams, Division of Hematology/Oncology, Children's Hospital Boston, 300 Longwood Ave, Karp Family Research Laboratories 08125.3, Boston, MA 02115; e-mail: dawilliams@childrens.harvard.edu.

References

1. Chiorazzi N, Rai KR, Ferrarini M. Chronic lymphocytic leukemia. *N Engl J Med.* 2005;352(8):804-815.
2. Panayiotidis P, Jones D, Ganeshaguru K, Foroni L, Hoffbrand AV. Human bone marrow stromal cells prevent apoptosis and support the survival of chronic lymphocytic leukaemia cells in vitro. *Br J Haematol.* 1996;92(1):97-103.
3. Schmid C, Isaacson PG. Proliferation centres in B-cell malignant lymphoma, lymphocytic (B-CLL): an immunophenotypic study. *Histopathology.* 1994;24(5):445-451.
4. Patten PE, Buggins AG, Richards J, et al. CD38 expression in chronic lymphocytic leukemia is regulated by the tumor microenvironment. *Blood.* 2008;111(10):5173-5181.
5. Tsukada N, Burger JA, Zvaifler NJ, Kipps TJ. Distinctive features of "nurselike" cells that differentiate in the context of chronic lymphocytic leukemia. *Blood.* 2002;99(3):1030-1037.
6. Burger JA, Tsukada N, Burger M, Zvaifler NJ, Dell'Aquila M, Kipps TJ. Blood-derived nurse-like cells protect chronic lymphocytic leukemia B cells from spontaneous apoptosis through stromal cell-derived factor-1. *Blood.* 2000;96(8):2655-2663.
7. Burkle A, Niedermeier M, Schmitt-Graff A, Wierda WG, Keating MJ, Burger JA. Overexpression of the CXCR5 chemokine receptor, and its ligand, CXCL13 in B-cell chronic lymphocytic leukemia. *Blood.* 2007;110(9):3316-3325.
8. Redondo-Munoz J, Jose Terol M, Garcia-Marco JA, Garcia-Pardo A. Matrix metalloproteinase-9 is up-regulated by CCL21/CCR7 interaction via extracellular signal-regulated kinase-1/2 signaling and is involved in CCL21-driven B-cell chronic lymphocytic leukemia cell invasion and migration. *Blood.* 2008;111(1):383-386.
9. del Pozo MA, Vicente-Manzanares M, Tejedor R, Serrador JM, Sanchez-Madrid F. Rho GTPases control migration and polarization of adhesion molecules and cytoskeletal ERM components in T lymphocytes. *Eur J Immunol.* 1999;29(11):3609-3620.
10. Chae HD, Lee KE, Williams DA, Gu Y. Cross-talk between RhoH and Rac1 in regulation of actin cytoskeleton and chemotaxis of hematopoietic progenitor cells. *Blood.* 2008;111(5):2597-2605.
11. Tomar A, Schlaepfer DD. Focal adhesion kinase: switching between GAPs and GEFs in the regulation of cell motility. *Curr Opin Cell Biol.* 2009;21(5):676-683.
12. Dallery-Prudhomme E, Roumier C, Denis C, Preudhomme C, Kerckaert JP, Galiegue-Zouitina S. Genomic structure and assignment of the RhoH/TTF small GTPase gene (ARHH) to 4p13 by in situ hybridization. *Genomics.* 1997;43(1):89-94.
13. Preudhomme C, Roumier C, Hildebrand MP, et al. Nonrandom 4p13 rearrangements of the RhoH/TTF gene, encoding a GTP-binding protein, in non-Hodgkin's lymphoma and multiple myeloma. *Oncogene.* 2000;19(16):2023-2032.
14. Pasqualucci L, Neumeister P, Goossens T, et al. Hypermutation of multiple proto-oncogenes in B-cell diffuse large-cell lymphomas. *Nature.* 2001;412(6844):341-346.
15. Hiraga J, Katsumi A, Iwasaki T, et al. Prognostic

analysis of aberrant somatic hypermutation of RhoH gene in diffuse large B cell lymphoma. *Leukemia.* 2007;21(8):1846-1847.

16. Gu Y, Chae H, Siefring J, Jasti A, Hildeman D, Williams DA. RhoH, a GTPase recruits and activates Zap70 required for T cell receptor signaling and thymocyte development. *Nat Immunol.* 2006; 7(11):1182-1190.
17. Chae HD, Siefring JE, Hildeman DA, Gu Y, Williams DA. RhoH regulates subcellular localization of ZAP-70 and Lck in T cell receptor signaling. *PLoS One.* 2010;5(11):e13970.
18. Chae HD, Siefring JE, Hildeman DA, Gu Y, Williams DA. RhoH regulates subcellular localization of ZAP-70 and Lck in T cell receptor signaling. *PLoS One.* 2010;5(11):e13970.
19. Dorn T, Kuhn U, Bungartz G, et al. RhoH is important for positive thymocyte selection and T-cell receptor signaling. *Blood.* 2007;109(6):2346-2355.
20. Sanchez-Aguilera A, Rattmann I, Drew DZ, et al. Involvement of RhoH GTPase in the development of B-cell chronic lymphocytic leukemia. *Leukemia.* 2010;24(1):97-104.
21. Bichi R, Shinton SA, Martin ES, et al. Human chronic lymphocytic leukemia modeled in mouse by targeted TCL1 expression. *Proc Natl Acad Sci U S A.* 2002;99(10):6955-6960.
22. Gu Y, Jasti AC, Jansen M, Siefring JE. RhoH, a hematopoietic-specific Rho GTPase, regulates proliferation, survival, migration, and engraftment of hematopoietic progenitor cells. *Blood.* 2005; 105(4):1467-1475.
23. Vissers JL, Hartgers FC, Lindhout E, Figdor CG, Adema GJ. BLC (CXCL13) is expressed by different dendritic cell subsets in vitro and in vivo. *Eur J Immunol.* 2001;31(5):1544-1549.
24. Kim H, Lee J, Hyun JW, Park JW, Joo HG, Shin T. Expression and immunohistochemical localization of galectin-3 in various mouse tissues. *Cell Biol Int.* 2007;31(7):655-662.
25. Butcher EC, Picker LJ. Lymphocyte homing and homeostasis. *Science.* 1996;272(5258):60-66.
26. Scielzo C, Bertilaccio MT, Simonetti G, et al. HS1 has a central role in the trafficking and homing of leukemic B cells. *Blood.* 2010;116(18):3537-3546.
27. Hartmann TN, Grabovsky V, Wang W, et al. Circulating B-cell chronic lymphocytic leukemia cells display impaired migration to lymph nodes and bone marrow. *Cancer Res.* 2009;69(7):3121-3130.
28. Ma Q, Jones D, Springer TA. The chemokine receptor CXCR4 is required for the retention of B lineage and granulocytic precursors within the bone marrow microenvironment. *Immunity.* 1999; 10(4):463-471.
29. Ansel KM, Harris RB, Cyster JG. CXCL13 is required for B1 cell homing, natural antibody production, and body cavity immunity. *Immunity.* 2002;16(1):67-76.
30. Shulman Z, Shinder V, Klein E, et al. Lymphocyte crawling and transendothelial migration require chemokine triggering of high-affinity LFA-1 integrin. *Immunity.* 2009;30(3):384-396.
31. Cancelas JA, Jansen M, Williams DA. The Role of Chemokine Activation of Rac GTPases in hematopoietic stem cell marrow homing, retention and peripheral mobilization. *Exp Hematol.* 2006; 34(8):976-985.
32. Ridley AJ, Schwartz MA, Burridge K, et al. Cell migration: integrating signals from front to back. *Science.* 2003;302(5651):1704-1709.
33. Wang H, Zeng X, Fan Z, Lim B. RhoH plays distinct roles in T-cell migrations induced by different doses of SDF1 alpha. *Cell Signal.* 2010;22(7): 1022-1032.
34. Mitra SK, Hanson DA, Schlaepfer DD. Focal adhesion kinase: in command and control of cell motility. *Nat Rev Mol Cell Biol.* 2005;6(1):56-68.
35. Pleyer L, Egle A, Hartmann TN, Greil R. Molecular and cellular mechanisms of CLL: novel therapeutic approaches. *Nat Rev Clin Oncol.* 2009; 6(7):405-418.
36. Ferrajoli A, Lee BN, Schlette EJ, et al. Lenalidomide induces complete and partial remissions in patients with relapsed and refractory chronic lymphocytic leukemia. *Blood.* 2008;111(11):5291-5297.
37. Chen CI, Bergsagel PL, Paul H, et al. Single-agent lenalidomide in the treatment of previously untreated chronic lymphocytic leukemia. *J Clin Oncol.* 2011;29(9):1175-1181.
38. Xu Y, Li J, Ferguson GD, et al. Immunomodulatory drugs reorganize cytoskeleton by modulating Rho GTPases. *Blood.* 2009;114(2):338-345.
39. Orchard JA, Ibbotson RE, Davis Z, et al. ZAP-70 expression and prognosis in chronic lymphocytic leukaemia. *Lancet.* 2004;363(9403):105-111.
40. Burger JA, Burger M, Kipps TJ. Chronic lymphocytic leukemia B cells express functional CXCR4 chemokine receptors that mediate spontaneous migration beneath bone marrow stromal cells. *Blood.* 1999;94(11):3658-3667.
41. Burger M, Hartmann T, Krome M, et al. Small peptide inhibitors of the CXCR4 chemokine receptor (CD184) antagonize the activation, migration, and antiapoptotic responses of CXCL12 in chronic lymphocytic leukemia B cells. *Blood.* 2005;106(5):1824-1830.
42. Mohle R, Failenschmid C, Bautz F, Kanz L. Overexpression of the chemokine receptor CXCR4 in B cell chronic lymphocytic leukemia is associated with increased functional response to stromal cell-derived factor-1 (SDF-1). *Leukemia.* 1999; 13(12):1954-1959.
43. Siveen KS, Kuttan G. Role of macrophages in tumour progression. *Immunol Lett.* 2009;123(2): 97-102.
44. Wu QL, Buhtoiarov IN, Sondel PM, Rakhmilevich AL, Ranheim EA. Tumoricidal effects of activated macrophages in a mouse model of chronic lymphocytic leukemia. *J Immunol.* 2009;182(11): 6771-6778.
45. Till KJ, Harris RJ, Linford A, Spiller DG, Zuzel M, Cawley JC. Cell motility in chronic lymphocytic leukemia: defective Rap1 and alphaLbeta2 activation by chemokine. *Cancer Res.* 2008;68(20): 8429-8436.
46. Li X, Bu X, Lu B, Avraham H, Flavell RA, Lim B. The hematopoiesis-specific GTP-binding protein RhoH is GTPase deficient and modulates activities of other Rho GTPases by an inhibitory function. *Mol Cell Biol.* 2002;22(4):1158-1171.
47. Cherry LK, Li X, Schwab P, Lim B, Klickstein LB. RhoH is required to maintain the integrin LFA-1 in a nonadhesive state on lymphocytes. *Nat Immunol.* 2004;5(9):961-967.
48. Worthylake RA, Burridge K. RhoA and ROCK promote migration by limiting membrane protrusions. *J Biol Chem.* 2003;278(15):13578-13584.
49. Xu J, Wang F, Van Keymeulen A, et al. Divergent signals and cytoskeletal assemblies regulate self-organizing polarity in neutrophils. *Cell.* 2003; 114(2):201-214.
50. Gardiner EM, Pestonjamasp KN, Bohl BP, Chamberlain C, Hahn KM, Bokoch GM. Spatial and temporal analysis of Rac activation during live neutrophil chemotaxis. *Curr Biol.* 2002; 12(23):2029-2034.
51. Tsuji T, Ishizaki T, Okamoto M, et al. ROCK and mDia1 antagonize in Rho-dependent Rac activation in Swiss 3T3 fibroblasts. *J Cell Biol.* 2002; 157(5):819-830.
52. Tilghman RW, Slack-Davis JK, Sergina N, et al. Focal adhesion kinase is required for the spatial organization of the leading edge in migrating cells. *J Cell Sci.* 2005;118(Pt 12):2613-2623.
53. Awan FT, Johnson AJ, Lapalombella R, et al. Thalidomide and lenalidomide as new therapeutics for the treatment of chronic lymphocytic leukemia. *Leuk Lymphoma.* 2010;51(1):27-38.
54. Lapalombella R, Andritsos L, Liu Q, et al. Lenalidomide treatment promotes CD154 expression on CLL cells and enhances production of antibodies by normal B cells through a PI3-kinase-dependent pathway. *Blood.* 2010;115(13):2619-2629.
55. Andritsos LA, Johnson AJ, Lozanski G, et al. Higher doses of lenalidomide are associated with unacceptable toxicity including life-threatening tumor flare in patients with chronic lymphocytic leukemia. *J Clin Oncol.* 2008;26(15):2519-2525.
56. Kurtova AV, Balakrishnan K, Chen R, et al. Diverse marrow stromal cells protect CLL cells from spontaneous and drug-induced apoptosis: development of a reliable and reproducible system to assess stromal cell adhesion-mediated drug resistance. *Blood.* 2009;114(20):4441-4450.